NASA/TM—1999-209053

3–D Surface Depression Profiling Using High Frequency Focused Air-Coupled Ultrasonic Pulses

Don J. Roth, Harold E. Kautz, and Phillip B. Abel
Glenn Research Center, Cleveland, Ohio

Mike F. Whalen and J. Lynne Hendricks
Sonix, Inc., Springfield, Virginia

James R. Bodis
Cleveland State University, Cleveland, Ohio

May 1999

The NASA STI Program Office . . . in Profile

Since its founding, NASA has been dedicated to the advancement of aeronautics and space science. The NASA Scientific and Technical Information (STI) Program Office plays a key part in helping NASA maintain this important role.

The NASA STI Program Office is operated by Langley Research Center, the Lead Center for NASA's scientific and technical information. The NASA STI Program Office provides access to the NASA STI Database, the largest collection of aeronautical and space science STI in the world. The Program Office is also NASA's institutional mechanism for disseminating the results of its research and development activities. These results are published by NASA in the NASA STI Report Series, which includes the following report types:

- TECHNICAL PUBLICATION. Reports of completed research or a major significant phase of research that present the results of NASA programs and include extensive data or theoretical analysis. Includes compilations of significant scientific and technical data and information deemed to be of continuing reference value. NASA's counterpart of peer-reviewed formal professional papers but has less stringent limitations on manuscript length and extent of graphic presentations.

- TECHNICAL MEMORANDUM. Scientific and technical findings that are preliminary or of specialized interest, e.g., quick release reports, working papers, and bibliographies that contain minimal annotation. Does not contain extensive analysis.

- CONTRACTOR REPORT. Scientific and technical findings by NASA-sponsored contractors and grantees.

- CONFERENCE PUBLICATION. Collected papers from scientific and technical conferences, symposia, seminars, or other meetings sponsored or cosponsored by NASA.

- SPECIAL PUBLICATION. Scientific, technical, or historical information from NASA programs, projects, and missions, often concerned with subjects having substantial public interest.

- TECHNICAL TRANSLATION. English-language translations of foreign scientific and technical material pertinent to NASA's mission.

Specialized services that complement the STI Program Office's diverse offerings include creating custom thesauri, building customized data bases, organizing and publishing research results . . . even providing videos.

For more information about the NASA STI Program Office, see the following:

- Access the NASA STI Program Home Page at ***http://www.sti.nasa.gov***

- E-mail your question via the Internet to help@sti.nasa.gov

- Fax your question to the NASA Access Help Desk at (301) 621-0134

- Telephone the NASA Access Help Desk at (301) 621-0390

- Write to:
  NASA Access Help Desk
  NASA Center for AeroSpace Information
  7121 Standard Drive
  Hanover, MD 21076

NASA/TM—1999-209053

3–D Surface Depression Profiling Using High Frequency Focused Air-Coupled Ultrasonic Pulses

Don J. Roth, Harold E. Kautz, and Phillip B. Abel
Glenn Research Center, Cleveland, Ohio

Mike F. Whalen and J. Lynne Hendricks
Sonix, Inc., Springfield, Virginia

James R. Bodis
Cleveland State University, Cleveland, Ohio

National Aeronautics and
Space Administration

Glenn Research Center

May 1999

Acknowledgment

Funding for this work came from the NASA HITEMP and COMMTECH programs, and from Sonix, Inc.

Trade names or manufacturers' names are used in this report for identification only. This usage does not constitute an official endorsement, either expressed or implied, by the National Aeronautics and Space Administration.

Available from

NASA Center for Aerospace Information
7121 Standard Drive
Hanover, MD 21076
Price Code: A03

National Technical Information Service
5285 Port Royal Road
Springfield, VA 22100
Price Code: A03

3-D Surface Depression Profiling Using High Frequency Focused Air-Coupled Ultrasonic Pulses

Don J. Roth, Harold E. Kautz, and Phillip B. Abel
National Aeronautics and Space Administration
Glenn Research Center
Cleveland, OH 44135

and

Mike F. Whalen and J. Lynne Hendricks
Sonix, Inc.
Springfield, VA 22152

and

James R. Bodis
Cleveland State University
Cleveland, OH 44115

ABSTRACT

Surface topography is an important variable in the performance of many industrial components and is normally measured with diamond-tip profilometry over a small area or using optical scattering methods for larger area measurement. This article shows quantitative surface topography profiles as obtained using only high-frequency focused air-coupled ultrasonic pulses. The profiles were obtained using a profiling system developed by NASA Glenn Research Center and Sonix, Inc. (via a formal cooperative agreement). (The air transducers are available as off-the-shelf items from several companies.) The method is simple and reproducible because it relies mainly on knowledge and constancy of the sound velocity through the air. The air transducer is scanned across the surface and sends pulses to the sample surface where they are reflected back from the surface along the same path as the incident wave. Time-of-flight images of the sample surface are acquired and converted to depth / surface profile images using the simple relation ($d = V*t/2$) between distance (d), time-of-flight (t), and the velocity of sound in air (V). Air-coupled surface profilometry is applicable to plate-like and curved samples. In this article, results are shown for several proof-of-concept samples, plastic samples burned in microgravity on the STS-54 space shuttle mission, and a partially-coated cylindrical ceramic composite sample. Impressive results were obtained for all samples when compared with diamond-tip profiles and measurements from micrometers. The method is completely nondestructive, noninvasive, non-contact and does not require light-reflective surfaces.

INTRODUCTION

To interface with other solids, many surfaces are engineered via plating, coating, machining methods, etc. to produce a functional surface ensuring successful end products. Additionally, *subsurface* properties such as hardness, residual stress, deformation, chemical composition, and microstructure are often linked to surface characteristics. Surface topography, therefore, contains signatures of the surface and possibly links to volumetric properties, and as a result serves as a vital link between surface design, manufacturing, and performance (refs. 1,2). Hence, surface topography can be used to diagnose, monitor and control fabrication methods. Ref. 1 states that "it is becoming increasingly obvious that a full understanding of the link between surface topography and functional performance can only be realized if a 3-D (areal) approach to surface characterization is used."

Diamond-tipped profilometry is the usual method for obtaining 2-D (line) precision surface depression variation in material samples and can resolve variation in the angstrom regime (ref. 1). However, this method requires contact with the sample which can cause undesirable alterations to the sample surface if further characterization is required. Additionally, the method is very slow and impractical for obtaining detailed, large scan area profiles, and has limited (micron-scale) vertical depth range. Optical scattering provides a large area profiling capability but requires lasers, sometimes an array of detectors, a light-reflective surface, and also provides only limited (micron-scale) vertical depth range (ref. 3). Scanning probe microscopy can provide noncontact surface profiling methods but is applicable only up to the hundreds of microns level and is not practical for macro-topography or large area profiling (ref.1). Ultrasonic methods have shown potential for surface profiling in the micron resolution regime in both the amplitude (scattering) and time-of-flight (which provides a direct measurement of depth) mode as shown by ref. 4. Ref. 4 reported surface profiling results with depth resolution in the 1 to 40 μm range using *water-coupled* ultrasonics employing frequencies up to 30 MHz.

Profiling surfaces with only high frequency focused ultrasonic pulses in air (air-coupled ultrasonic method) offers the advantage of being useable in environments where stylus contact, laser impingement, or water immersion is undesirable or impractical. Additionally, as implemented in this study, it offers large-area scan capability and large (mm) vertical depth range, though not at the sub-micron characterization resolution level. The method currently resides as a user-friendly option within a commercially-available ultrasonic scan system and uses off-the-shelf ultrasonic air transducers. In the development of this method, the authors

1) concentrated solely on the time-of-flight method to obtain depth profiling by direct measurement

2) used 13-bit computer technology at 1 GHz analog-to-digital sampling rate to allow depth profiling over significantly larger ranges than has been available to date (see Appendix A). This allows a 32x increase in depth range (~ 1.4 mm depth range) with no decrease in time resolution as compared to 8-bit data gates (~ 0.04 depth range)

[see Appendix A]. It is conceivable that the 8192 point data acquisition limit will be increased in the future.

3) demonstrated the use of the system for surface profiling on a cylindrical component as well as plate-like samples.
4) developed capabilities for:
   a) on-line areal analysis to allow cursor measurement of surface depression at any location on the profile
   b) leveling
   c) Three-dimensional (3-D) as well as Two-dimensional (2-D) graphic displays of the profiles
   d) image processing capability (such as removal of faulty data and replacement by the average of nearest neighbors, and preliminary low pass filtering)
   e) exportation of the data into different spreadsheet formats for off-line processing

In this article, results are shown for several proof-of-concept samples (an embossed superman logo, Kennedy half-dollar, and wedge-shaped ceramic sample), plastic samples burned in microgravity on the STS-54 space shuttle mission, and a partially-coated cylindrical ceramic composite sample.

BASIC PRINCIPLES

Obtaining Surface Profiles from Time-of-Flight Information

The ultrasonic profiling method uses an ultrasonic focused beam as a stylus with the beam impinging on the sample surface at nominally-perpendicular incidence as shown in figure 1. Time-of-flight images using a 13-bit data gate are used to allow fine time resolution over significant surface depressions. Surface depression profiles are calculated based on the time-of-flight images. The method relies mainly on knowledge of the velocity of ultrasound through air which remains reasonably constant at all times and locations if temperature is held constant (as in the air of a temperature-regulated room). The method as implemented on the Sonix, Inc. Flexscan ultrasonic c-scan system (ref. 5) using the Sonix STR*81GU analog-to-digital converter board, has potential for extremely high speed. The sample should be placed on a support of uniform flatness and parallelness but provisions in the commercial software allow releveling of the initial surface profile as is common in most commercially-available diamond-tip profilometers.

In figure 1, $d_{x,y}$ is the distance at any x,y location between the sample and the ultrasonic transducer and is variable due to the surface irregularity. If the ultrasonic system is activated and an x,y ultrasonic scan is performed over the sample, ultrasonic reflections off of the top sample surface will be obtained. Normalized surface depression at any x,y location ($Z_{x,y}$) is determined from:

$$Z_{x,y} = \frac{V_{air}}{2}(t_{x,y} - t_{\min}) \quad (1)$$

where $t_{x,y}$ is the time-of-flight of the first front surface reflection at any x,y surface location (and will vary with $Z_{x,y}$ and $d_{x,y}$), t_{min} is the time-of-flight corresponding to the highest surface position on the sample front surface, and V_{air} is the velocity of ultrasound in air (dependent upon the temperature and is ~ 0.34 mm/μsec at 68°F in dry still air).

Echo Features used for Time-of-Flight

It is recommended that the precise time-of-flight of the front surface echoes is measured either to the intersection of a gate and the leading edge of the echo (the height level of the gate being set by the user), or by gating a selected peak of the echo (again determined by the user). These cases are illustrated in figure 2 where gated front surface echoes are shown on the digital oscilloscope display present on the Sonix Flexscan interface. Gating the leading edge has generally produced better results than gating the peak and is recommended.

EXPERIMENTAL PROCEDURE

Materials

First, to benchmark the depth resolution and quantitative accuracy of the ultrasonic air profiling system at 1 MHz, an aluminum step wedge was fabricated having steps separated in depth by 24, 50, 83, 104, and 200 μm, respectively. The machining deviation for the steps was ± 2 μm. Secondly, to benchmark the lateral resolution capability of the ultrasonic air profiling system at 1 MHz, an aluminum block was manufactured with a series of channels separated by increasing distance. The channels were separated by 0, 37, 96, 101, 113, 120, 130, 157, 177, 236, 283, 381, 484 and 577 μm. The machining deviation for the channel separation was ± 10 μm. Then, several proof of concept samples were profiled which included a ceramic wedge sample having a smooth ~ 300 μm thickness gradient from left-to-right edge, an embossed superman logo, and a Kennedy half-dollar coin (figure 3). The next samples profiled were “real world” samples that required knowledge of surface depression information. Of these, the first was a set of two small (~ 0.6 cm by ~ 3 cm) plastic samples that were the object in a microgravity combustion space experiment onboard the space shuttle (mission STS-54). It was desired to obtain whole area surface depression profiles to characterize the microgravity burning of these samples. Figure 4 shows several diamond tip profilometry line scans across the surface of one of the burned plastic samples. The burn was started at the right end of the sample. The burn caused 1) a loss of material from the 23 to the 15 mm locations and 2) a lip to form at the ~ 15 mm mark that was ~ 0.2 mm higher than the starting surface height. The last sample profiled in this investigation was a portion of a cylindrical ceramic composite structure of potential use as a liner in a high-temperature combustion system (figures 5a and 5b). It contained a thin coating of protective barrier material on

the outer surface, a rough surface due to the weave geometry, and various seams and grooves resulting from manufacture. The latter was profiled to show the potential feasibility of air profiling curved or cylindrical structures.

Ultrasonic Profiling

Ultrasonic time-of-flight c-scans were performed on all samples with a Sonix ultrasonic scan system with a screw-driven motorized bridge assembly. For the scans, an Ultran Labs 1 MHz nominal center frequency broadband transducer of focal length = 5.08 cm (2 in.) and element diameter = 2.54 cm (1 in.) was employed. Actual center frequency (as obtained from the magnitude plot of the discrete fourier transform) for pulses reflected from the front surface of an aluminum plate placed at the focal distance was ~ 0.73 MHz. 1 GHz a/d sampling rate and 13-bit (8192 bits) time-of-flight data gates were employed. (The 13-bit computer technology was specifically developed to allow longer gates with no decrease in time resolution. See Appendix A.) Nominally-predicted focal spot size (indicating the area of surface sampled in one measurement) was ~ 1.7 mm (see Appendix B). Scan (length) and step (width) increments used for the plate-like samples were 95 μm, significantly smaller than the predicted focal spot size in hopes of obtaining finer averaged lateral detail as was done in prior ultrasonic studies (refs. 4,6). Scans were on the order of 400 scan points by 400 scan lines. Using the Sonix STR*81GU analog-to-digital (A/D) converter board, linear scan speeds were on the order of 5 mm/sec at the 95 μm scan / step increment with 4 waveform averages performed in software as the scan progressed. (Waveform averaging “on-the-fly” using the sum of four successive waveform acquisitions was used to obtain higher signal-to-noise ratios at the expense of scan speed.) A Panametrics 5055PR pulser-receiver (10 MHz bandwidth) was used to pulse the transducer and receive the ultrasonic signal, and to trigger the A/D board. The settings on the pulser-receiver were energy = 2, attenuation = 0 dB, High Pass (H.P.) Filter = out, Gain = 40 dB, and Damping = 2. The signal out of the 5055PR was sent into a Physical Acoustics 1220A preamplifier set at 60 dB, and the output from the preamplifier was connected to a Physical Acoustics AE1A amplifier set at 15 dB.

Figure 5c shows the experimental configuration used to profile a portion of the inner surface of the ceramic composite cylinder. A turntable scan was performed with a 0.2^{o} scan (cylindrical) increment and 0.2 mm step (height) increment employed for the cylinder. For profiling of a portion of the outer surface, the manipulator arm was positioned outside the cylinder with the transducer facing the outer surface while scan and step increments were the same as for profiling the inner portion. (For air profiling to be accurate on curved or cylindrical structures, the structure must be perfectly in round and be perfectly centered on the spinning turntable. The latter was accomplished to the greatest degree possible. A measure of out-of-roundness of the cylindrical structure can be gauged if in fact it is perfectly centered on the turntable.)

During initial set-up, the transducer was precisely focused at the sample front surface (in a mid-region of the sample) by adjusting its distance from the sample and by adjusting its gimbal angle to obtain the time location where the highest amplitude for the front-surface–reflected echo occurred on the digital oscilloscope. (The variations in focal

length caused by surface depressions in the sample did not appear to significantly affect results.) A single data gate was used intersecting the negative leading edge of the front surface-reflected echo (rf waveform display) which was heavily driven into saturation (over 100% full scale height of the oscilloscope display) similar to what is shown in figure 2a. Gate length was set to cover the entire time extent corresponding to the surface variation being tracked. Air temperature was $71^{o}F \pm 1^{o}F$.

Using eq. (1), surface depression profiles were calculated from raw time-of-flight images obtained from the leading edge-gated front surface echo. Appendix C shows the user interface for the commercial ultrasonic profilometry system and provides detailed procedures for the user for processing front surface echo time-of-flight images to obtain surface depression profiles. Sample profile images were leveled as needed by subtracting from the sample time-of-flight scan an identical scan of the support plate (figure 1) on which the sample sat. (A future leveling option will involve subtraction of a plane obtained from planar regresssion and require only one scan.) Profile results are presented in both 2-D and 3-D image displays as obtained directly from the Sonix system. Appropriate 8-bit (256 levels) color schemes are chosen to highlight the results. Removal of extreme high and low values caused by randomly improper gating was performed where necessary using an option in the surface profilometry system. At these locations, nearest neighbors averaging was implemented to replace the value. In general, eight nearest valid neighbors are used in used in the calculation of the average. Exportation of the data for off-line processing is an option in the software so that one can use his or her preferred image processing and display package.

RESULTS AND DISCUSSION

Aluminum Step Wedge & Channeled Aluminum Block: Resolution Capability

The air-coupled surface profile and a typical line profile for the aluminum step wedge are shown in figure 6a. The individual steps as small as 24 ± 2 μm (the smallest step) are resolved as shown by the color differences of the regions and the step heights shown on the line profile. An oscillating background noise on average of ~ 10 μm is superimposed on the line profile and image and will be discussed more in the results below on the ceramic wedge and in Appendix A. Table I compares the mean values from the ultrasonically-derived surface depression map with that obtained from micrometer measurements. The mean values were obtained by drawing a best fit horizontal line through the oscillating line profile of each individual step section. In this manner, an equal “amount” of deviation was placed above and below the line. Good agreement is observed between measurements obtained from micrometers and from those obtained ultrasonically.

Table I.—Comparison of surface depression magnitude from ultrasonic scan and micrometer measurements in the stepped Aluminum block.

Step	Step-to-Step Surface Depression from Micrometer Measurement (μm)	Step-to-Step Mean Surface depression from Ultrasonic Scan (μm)
A	24	30
B	50	47
C	83	85
D	104	95
E	207	215

The front surface time-of-flight air ultrasonic image for the channeled aluminum block is shown in figure 6b which revealed the lateral resolution available with the experimental configuration of this study. The third and fourth channels from the right were clearly resolved. These channels were separated by 381 μm indicating the lateral resolution of this method to be ~ 400 μm. This was ~ 1/4th the nominally-predicted focal spot size (see Appendix B).

Ceramic Wedge

Figure 7a shows the air-coupled surface profile of the ceramic wedge and a line profile for one scan line. Although the sample had a smooth thickness gradient, a color table consisting of only five shades was used so as to facilitate comparison with figure 7b. Maximum surface depression is ~ 300 – 400 μm, depending on the locations sampled. (A global statistical maximum using the whole data set is not valid because of edge effects). This compares with 300 μm measured by micrometers. The line profile has a superimposed vertical "noise" effect of ~ 10 – 40 μm as pointed out in figure 7a. For comparison, figure 7b shows a thickness map of the ceramic wedge obtained from immersion ultrasonic velocity measurements at 20 MHz (ref. 7) and an associated line profile at ~ the same location. For the latter, maximum surface depression is ~ 300 – 320 μm. The latter also shows a smoother line profile, with little vertical noise superimposed onto the line profile of figure 7b. The superimposed noise in the line profile of figure 7a is due to time-related "jitter" (oscillation) and was estimated at ~ ± 200 ηsec from measurements off of the digital oscilloscope. As discussed in more detail in Appendix A, the jitter is probably what limits the depth resolution at this time to ~ 25 μm. Another undesirable feature apparent in the profile image of figure 7a is the "bands of noise" or "waviness." This feature is prevalent in all images in this study in which waveform averaging was performed; the reason that waveform might have caused this effect is unknown. Subtraction of sample and support time-of-flight scans were unsuccessful in eliminating the feature which indicates its "irregularity." It is likely that customized filtering operations can remove much of this effect. (In typical profilometry

systems, low-pass filtering historically has been used to eliminate the longer wavelength (form and waviness) components (refs. 1,2)). In spite of this feature, however, the maximum surface depression magnitude of ~ 300 – 400 μm obtained from air-coupled profiling compares well with that obtained from micrometer and immersion ultrasonic velocity measurements.

Embossed Superman Logo and Kennedy Half-dollar

Figures 8 and 9 show 2-D and 3-D views of air-coupled surface profiles for the embossed superman logo and the Kennedy half-dollar, respectively. The 3-D views (figures 8b and 9b) clearly show the topographical features of both samples. The “bands of noise” feature may cause some inaccuracy in quantitative evaluation of surface depressions, and causes some “waviness” in the three-dimensional images, but the relative heights of the features are represented clearly. Measurements off of the air-coupled surface profile for the coin revealed a surface depression maximum ~ 200 – 250 μm which agreed well with touch probe maximum depression measurements (similar to micrometer) of ~ 250 μm. Measurements off of the air-coupled surface profile for the superman logo revealed a surface depression maximum ~ 700 μm which agreed well with touch probe maximum depression measurements of ~ 720 μm.

Burned Space Experiment Sample

Figure 10 shows 2-D and 3-D views of air-coupled surface profiles for the burned space experiment samples and a line profile across one of them. The 3-D view (figure 10b) and line profile from figure 10a clearly show the topographical features of both pieces, including the small hump formed by the burn. Measurements off of the air-coupled surface profile for the top sample revealed a surface depression range ~ 800 μm which agreed well with the diamond-tip profile results showing ~ 700 – 800 μm maximum depression. Both samples showed a similar air-coupled surface burn profile.

Ceramic Composite Cylinder

Figures 11 and 12 show two-dimensional surface profiles of the outer and inner regions, respectively, of the ceramic composite cylinder portions profiled. The profiles are "unwrapped" images revealing the entire 360° scan. Coating thickness from the outer cylinder air-coupled surface profile (figure 11) was measured at ~ 250 μm, which compared reasonably well with ~ 200 μm value measured using a touch probe. Also shown on this image is the regular pattern of structure thickness variation (seen as bumps) resulting from manufacture. Representative grooving on the inner portion was measured on the air-coupled surface profile at 300 - 500 μm which compared well with values obtained from caliper measurements. The slope in the line profile also clearly reveals an out-of-roundness condition mainly due to set-up of the cylinder on the spinning turntable. As previously stated, the structure must be perfectly in round and be perfectly centered on the spinning turntable to eliminate out-of-roundness indication. Customized low-pass filtering methods would likely be effective at removing this type of

indication since it is essentially a long-wavelength condition. Conversely, this air-coupled profiling method can be used to determine the out-of-roundness and off-center condition.

FURTHER THOUGHTS

Much higher speeds are possible with no waveform averaging or with hardware waveform averaging. Additionally, quality is not greatly degraded with no waveform averaging (resulting in much greater scan speeds). For example, the profile of figure 13b was obtained at a scan speed nearly 20x greater than that for the profile of figure 13a / figure 9b with little loss in quality.

For the highest precision measurement, freedom from external vibration and that due to motor / bridge assembly movement and electrical noise is important so that the waveform received at the transducer is as stable as possible. These issues are discussed in further detail in Appendix A.

FUTURE DIRECTIONS

The authors have identified several potential areas for improvement for this method. These include 1) the use of higher frequency air transducers if they become available to increase the spatial (lateral) resolution capability, 2) the application of vibration isolation methods to reduce jitter and thereby increase depth resolution capability and 3) the development and application of customized low-pass filtering to filter out any waviness from the profiles of plate-like and cylindrical samples. Solutions to air current sensitivity (turbulence) are probably the most pressing need.

CONCLUSIONS

Surface topography is an important variable in the performance of many industrial components and is normally measured with diamond-tip profilometry over a small area or using optical scattering methods for larger area measurement. This article showed quantitative surface topography profiles as obtained using only high-frequency, focused ultrasonic pulses in air. Recommended air transducers to generate the air pulses are ~ 1 MHz nominal center frequency. The method is simple and reproducible because it relies mainly on knowledge and constancy of the sound velocity through the air. The air transducer was scanned across the surface and sends pulses to the sample surface where they are reflected back from the surface along the same path as the incident wave. Time-of-flight images of the sample surface are acquired and converted to depth / surface profile images using the simple relation ($d = V*t/2$) between distance (d), time-of-flight (t), and the velocity of sound in air (V). The system has the ability to resolve surface depression variations as small as 25 μm with 400 μm lateral resolution, is useable over a 1.4 mm vertical depth range, and can profile large areas only limited by the scan limits of the particular ultrasonic system. (Best-case depth resolution is 0.25 microns which may

be achievable with improved isolation from air currents and vibration [external and that due to motor / bridge assembly movement].) The method using an optimized configuration is reasonably rapid and has all quantitative analysis facilities on-line including two- and three-dimensional visualization capability, extreme value filtering (for faulty data), and leveling capability. Air-coupled ultrasonic surface profilometry is applicable to plate-like and curved samples. In this article, results were shown for several proof-of-concept samples, plastic samples burned in microgravity on the STS-54 space shuttle mission, and a partially-coated cylindrical ceramic composite sample. Impressive topographical representations were obtained for all samples when compared with diamond-tip profiles and measurements from micrometers. The method is completely nondestructive, noninvasive, non-contact and does not require light-reflective surfaces.

APPENDIX A

Time and Distance Resolution Determination for the Commercial Implementation

This section explains the time resolution determination for the commercial scan system employed in this investigation and the significant advantage that 13-bit time-of-flight data gates have over 8-bit gates. Units employed in this analysis are those commonly used in ultrasonics and are shown in the equations of this section where appropriate. Time resolution (TR) of the ultrasonic data acquisition for the commercial scan system employed in this investigation can be defined in terms of analog-to-digital (a/d) sampling rate (SR), gate length in points (GL), and number of data bits available (n) for the gate according to:

$$TR(\eta\,\mathrm{sec}) = \left(\frac{1}{SR[GHz]}\right) \tag{A1}$$

for 8-bit data gate length (GL) ≤ 256 points and for 13-bit data gate length (GL) ≤ 8192 points and

$$TR(\eta\,\mathrm{sec}) = \left(\frac{GL[pts]}{2^n}\right)\left(\frac{1}{SR[GHz]}\right) \tag{A2}$$

for 8-bit data gate lengths (GL) >256 points and for 13-bit data gate length (GL) > 8192 points. For example, equation (A2) shows that gate lengths longer than 256 points will degrade the time resolution for 8-bit data gate lengths. Figure A1a shows time resolution (TR) versus gate length (GL) in points under the conditions defined by eqs. (A1) and (A2). For example, for a 13-bit data gate ≤ 8192 and 1 GHz a/d sampling rate, a time resolution (TR) of 1 ηsec is achieved.

Alternately, time resolution (TR) of the ultrasonic data acquisition can be defined in terms of analog-to-digital (a/d) sampling rate (SR), gate length (GL) in ηsec, and number of gate bits available (n) according to:

$$TR(n\ \mathrm{sec}) = \left(\frac{1}{SR[GHz]} \right) \tag{A3}$$

for 8-bit data gate, (a/d sampling rate (SR) [GHz])•(gate length (GL) [ηsec]) ≤ 256 and for 13-bit data gate, (a/d sampling rate (SR) [GHz])•(gate length (GL) [ηsec]) ≤ 8192 and

$$TR(n\,\mathrm{sec}) = \left(\frac{GL(\eta\,\mathrm{sec})}{GL_{\max}(\eta\,\mathrm{sec})} \right) \left(\frac{1}{SR[GHz]} \right) \tag{A4}$$

where Gl_{max} is the maximum gate length before resolution degrades (ηsec) and it occurs when: for 8-bit gate, (a/d sampling rate (SR) [GHz])•(gate length (GL) [ηsec]) >256 and for 13-bit gate, (a/d sampling rate (SR) [GHz])•(gate length (GL) [ηsec]) > 8192. Figure A1b shows time resolution versus gate length (GL) in ηsec under the conditions defined by eqs.(A3) and (A4).

Figures A1a and A1b show the gate lengths where time resolution begins to decrease beyond that set by the a/d sampling rate. *Gate lengths where time resolution begins to degrade beyond that set by the a/d sampling rate are normally never approached in practical scan set-ups when using 13-bit data gates.* 13-bit computer technology in the time mode was specifically developed to allow longer gates with no decrease in time resolution. For acquisition of echo features for a sample having significant surface depression variation, and when using high a/d sampling rates, long gates are normally necessary to follow the echo movement as sample surface depression changes. Hence, where long data gate lengths are necessary, it is important to employ 13-bit data gates for highest time resolution.

It is also necessary to keep in mind that the commercial scan system employed in this investigation has an 8192 data point (13-bit) acquisition limit at present; specifically, the first gate starting point subtracted from the last gate ending point must be less than 8192 points. With a 13-bit acquisition limit, the improvement in vertical depth range over which time / depth resolution stays constant is 32-fold as compared to a 8-bit acquisition limit. Specifically, for 1 GHz sampling rate (1 data point = 1 ηsec), dry still air at 68°F (V_{air} = 0.34 mm/μsec) (ref. 9, figure A2a), and vertical depth range = velocity*(maximum gate length in time [8192 ηsec])/2 in the pulse-echo configuration, a 1.393 mm vertical depth range is obtained with 8192 (13-bit) data point acquisition limit versus a 0.0435 mm vertical depth range obtained with a 256 (8-bit) data point acquisition limit.

Actual surface depression ($Z_{x,y}$) profiles are arrived at from the following equations:

$$Z_{x,y}(\mu m) = \frac{V_{air}(mm/\mu\sec)}{2} \bullet (TR(\eta\sec)) \bullet (DL_{x,y} - DL_{\max}) \tag{A5}$$

or, in terms of sampling rate:

$$Z_{x,y}(\mu m) = \frac{V_{air}(mm/\mu\sec)}{2} \bullet \left(\frac{1}{SR(GHz)}\right) \bullet (DL_{x,y} - DL_{\max}) \tag{A6}$$

where DL_{max} is 65,535 and $DL_{x,y}$ is the scaled data level at the x,y scan location. $DL_{x,y}$ is scaled to 16-bits (the 16-bit image option must be enabled) after acquisition to account for the fact that other a/d boards in the Sonix, Inc. product line use true16-bit data gates. The scaling is done according to:

$$DL_{x,y} = (t_{x,y}[pts.])65{,}535 / gate_length[pts.] \tag{A7}$$

where $t_{x,y}$ is the time location in points obtained from where the gate intersects the leading edge of the front surface waveform (or the time location of one of the front surface waveform peaks).

Distance / depth resolution (DR) for surface profiling is obtained to a first approximation from:

$$DR(\mu m) = \frac{V_{air}(mm/\mu\sec) \bullet TR(\eta\sec)}{2} \tag{A8}$$

For dry air at 68°F (V_{air} = 0.34 mm/μsec) (ref. 9, figure A2a), this time resolution translates into DR to a first approximation of ~ 0.17 μm from eq. (A8). The error in this value can be found by performing the traditional error analysis where (ref. 8):

$$\sigma_{DR} = \sqrt{\left(\frac{\partial(DR)}{\partial V_{air}}\right)^2 \sigma_{Vair}^{\ 2} + \left(\frac{\partial(DR)}{\partial(TR)}\right)^2 \sigma_{TR}^{\ 2}} \tag{A9}$$

The error in time resolution (TR) can be expressed in terms of the analog-to-digital sampling rate (SR) according to:

$$\sigma_{TR}(\eta\sec) = \frac{1}{2 \bullet SR(GHz)} \tag{A10}$$

so that for 1 GHz a/d sampling rate σ_{TR} = 0.5 ηsec. Using σ_{Vair} = 0.005 mm/μsec as the error in measuring air velocity (c), a $\sigma_{DR} \cong 0.08$ μm is obtained from eq. (A9). Adding this error to the result of eq. (A8) gives a best case (ideal conditions) estimate for vertical distance resolution (DR) of approximately 0.25 μm for 1 GHz sampling rate using air coupling.

This analysis does not take into account error due to electromagnetic interference that superimposes itself upon the signal, scattering effects that result in the front surface echo being intersected by the time gate in an inconsistent manner, a time-related "jitter" (oscillation) that was observed in the signal possibly due to vibration (external and that due to motor / bridge assembly movement) and air currents (from temperature and pressure variations), and other ultrasonic system-related effects. It is these factors that likely cause the most severe error in this method. Error due to electromagnetic interference can be minimized with signal averaging.

The time-related "jitter" (oscillation) observed in the signal was estimated at ~ ± 200 ηsec from measurements off of the digital oscilloscope **without the scanner moving**. The jitter is possibly due to vibration and air currents (from temperature and pressure variations). Reference 4 found turbulence from air currents prohibitive in his application of an air-coupled ultrasonic sensor for profiling rotating cylinders. Setting σ_{TR} = 200 ηsec and substituting this value into eq. (A8) gives $\sigma_{DR} \cong 33$ μm. This value was similar to the vertical "noise" superimposed upon a typical surface depression profile (figure 7a). At present, this effect appears to be the limiting factor in depth resolution. (Depth resolution was ~ 25 μm as shown in figure 6a). A thickness map of the ceramic wedge obtained from immersion ultrasonic velocity measurements at 20 MHz (ref. 7) shows a smoother line profile with little superimposed noise (figure 7b). Temperature effects on ultrasonic velocity in dry air were found to be small based on data obtained from ref. 9; a temperature variation from 68°F to 69°F was calculated to cause less than 0.1% velocity variation (see figure A2a). Humidity effects on ultrasonic velocity in air at 68 ^{o}F were found to be small as well (see figure A2b); a change in humidity from 70% to 80% was calculated to cause less than 0.1% velocity variation. Thus, the error in distance / depth resolution (eq. (A9)) should not be significantly affected by a few degrees of temperature variation or several percent of humidity variation. Vibration isolation methods need to be used to minimize the effects of vibration (external and that due to the motor / bridge assembly movement).

Another effect present in the resulting profile image was a "waviness" or "bands of noise" feature (figure 7a) that can potentially be low-pass filtered using customized methods (ref. 1,2). This feature was prevalent in all images in this study in which waveform averaging was performed and would also affect accurate measurement of surface depression. The reason that waveform averaging might have caused this effect is unknown. Further investigation is needed to minimize these errors so that depth resolution can be obtained on the micron scale.

Potentially, using different pulsing mechanisms and changes in transducer design can result in more highly-vertical leading edges thus minimizing the error caused by the front surface echo being intersected by the time gate in an inconsistent manner.

APPENDIX B

Transducer Focal Spot Size

Transducer focal spot diameter determines the area of the specimen surface sampled. It is likely to limit sample feature resolution, although complex scattering interactions of ultrasound off surface features closely spaced together may result in "improved" or worsened resolution. It is expected that the focal spot diameter would limit the lateral resolution capability. A relationship exists between focal spot diameter of an ultrasonic beam (ϕ) at 50% drop in sound pressure (- 6dB point), ultrasonic wavelength (λ), transducer focal length (L_f), and transducer element diameter (X) according to (ref. 10):

$$\varphi = 2.44 \bullet \lambda \bullet \frac{L_f}{X} \tag{B1}$$

Ultrasonic wavelength (λ) can be expressed in terms of transducer frequency and ultrasonic velocity in air (V_{air}) according to:

$$\lambda = \frac{V_{air}}{f} \tag{B2}$$

Noting that for dry still air, V_{air} = 0.34 mm/μsec at 68°F (ref. 9) and substituting eq. (B2) into eq. (B1) gives:

$$\varphi(\mu m) = 2440 \bullet \frac{0.34(mm/\mu\sec)}{f\,(MHz)} \bullet \frac{L_f\,(mm)}{X\,(mm)} \tag{B3}$$

Figures B1 and B2 show the relationship between focal spot size, transducer frequency, focal length, and element diameter. For example, for the transducers used in this experiment (1 MHz center frequency focused transducer with a focal length of 50.8 mm and element diameter 25.4 mm) a focal spot diameter of ~ 1.7 mm was predicted from eq. (B3) which is several orders of magnitude larger than that for typical diamond tip profilometers that have stylus diameters on the order of 4 μm. Laser systems achieve spot sizes on the order of 25 μm as well (ref. 3). The large focal spot size for the air stylus likely results in an averaged response over the testpiece area sampled (refs. 4,6).

APPENDIX C

Processing Front Surface Echo Time-Of-Flight Images To Obtain Surface Depression Profiles

This section describes in more detail the steps necessary to obtain quantitative ultrasonic surface profiles using the Sonix ultrasonic c-scan system and Flexscan software (present version is 4.71a). The user is expected to have reasonable knowledge of the Sonix c-scan system and Flexscan software, and is referred to the Sonix Flexscan User Manual (ref. 5) for more information.

1. Place sample on level, smooth surface support plate. In ‘configuration’ window from ‘Edit’ menu item, select ‘16-bit image type’ (see figure C1). In ‘feature parameters’ window from ‘Edit’ menu, select ‘peak-detection type = threshold’ and ‘time-of’flight to edge’ (see figure C2). In ‘scan set-up’ window under ‘Scan’ menu item, set up scan parameters (figure C3). Perform time-of-flight (TOF) ultrasonic scan for a front surface echo waveform off the sample as described in the Procedures section of this report. Make sure to increase the pulser-receiver gain so as to significantly threshold out the echo so as to have a consistent leading positive or negative edge that will be present at all scan positions (as is physically possible; it is recognized that extreme scatter may occur off very rough surfaces causing significant echo attenuation and leading either to no gate intersection with the echo or a significantly different intersection position along the leading edge) (see figure C4). Place time gate in position to intersect leading edge at desired location. At the scan origin, record the exact time-of-flight in μsec where the gate intersects the leading edge by expanding the digital oscilloscope so echo is highly spread apart, and using the ‘locate-measure’ cursor under the ‘Measure’ menu item to find this time. Record the z-motor position in mm. Save the image and parameter files.

2. For leveling in conjunction with surface profiles, remove the sample from the support and refocus the transducer at the scan origin onto the support plate by moving the z-axis down (keyboard control) until the leading edge of the front surface echo off of the support plate intersects the gate at the exact same time location (or as close as possible) as that for the scan on the sample. Perform identical scan as that for sample. Save the image and parameter files. Using the ‘Add/Subtract’ window (Image Combination) under the ‘Process’ menu item (see figure C5), mouse click on the sample TOF image (in the title bar) and then mouse click on ‘Image 1’ box in the ‘Image Combination’ window. Mouse click on the support scan image title bar and then click in ‘image 2’ field in the ‘Image Combination’ window. At the top of the ‘Image Combination’ window, mouse click on the mathematical operator box until a ‘-‘ appears indicating image subtraction. Click ‘process’ in the ‘Image Combination’ window to obtain a ‘leveled’ TOF image. Save the leveled image. This image will be of type .cs rather than .cs1.

3. Open ‘surface profilometry’ window under ‘Process’ menu item (see figure C6). Hit ‘return’ key to move between fields in this window. Mouse click on the third box

down from the top of window until ‘No Support Info’ is displayed. (Since leveling was accomplished with Add/Subtract function, we do not need to consider the support scan information here.) If desired, use mouse cursor to draw ‘rubber rectangle’ for processing of a sub-area of image rather than the whole image. To use ‘rubber rectangle’, hit middle mouse button until ‘cross’ is apparent and then drag mouse over desired area of sample scan to outline the area.

4. In ‘surface profilometry’ window, mouse click on sample TOF scan image title bar, then click on ‘surface scan’ box. Hit ‘return’ key until reaching ‘couplant velocity’ entry. Adjust temperature-dependent couplant velocity to the measured value or known value. Initially, have ‘no bkgd subst’ option enabled if no extreme value filtering is needed. Depending on whether sample fills image (no background area) or sample is on background, enable the appropriate option. If rubber rectangle is used, it is likely that it will encompass just a sample area (no background). Have ‘filter = off’ enabled if no extreme value filtering is needed. Enable ‘ascii output’ or ‘no ascii output’ depending on whether it is desired to work with data off-line. When ascii output is generated, 2 text files are created. These are a continuous text file for surface depression profile values (sura.asc) and a text file of columnar format having surface depression profile as a function of x,y scan coordinates (surc.asc). Mouse click on ‘begin processing’ in surface profilometry window which will generate the surface profile. Toggle on the units box in the upper right hand corner to see maps in terms of (μsec), mm or in. Save the surface depression profile image. This image will be of type .cs rather than .cs1.

5. If extreme value filtering is necessary, use ‘Clamp result’ and filter = ‘extreme value’ (see figure C8). Open the ‘Palette window’ from the ‘windows’ menu, mouse click on the S8 palette and add a hinge. Mouse click on ‘Thr’ button at the right of the Palette window to go into threshold mode. Initially, adjust the highest hinge upward so that it is at 100% and the lowest hinge to 0%. Then, adjust the highest hinge downward so that high extreme values to filter are made white and adjust the middle hinge either upward or downward so that low extreme values to filter are made black. Other colors can also be used for preferred visualization in a similar fashion. To use other colors for example, click on the top hinge, and make it red by moving center cursor notch in hexagon in palette window to the ‘R’ symbol. The slider control should be set at 100%. Then click on the bottom hinge and make blue by moving the center notch cursor in hexagon to the ‘B’ symbol. The slider control should be set at 100%.

   Then, in the surface profilometry window, adjust ‘clamp to palette min’ to the % associated with the middle hinge, and adjust the ‘clamp to palette max’ to the % associated with the upper hinge.

6. For samples having a donut-type configuration (hole in the middle) such as the Baaklini MMC rings, use ‘no bkgd subst’, ‘sample is on bkgd’ and ‘filter = off’. Filtering cannot be performed on this type of sample.

7. The ‘add/subtract’ (Image Combination) window can be used further for contrast expansions or adding / subtracting constant values for normalization.

8. Use ‘cross-section’ from the ‘Visualize’ menu item to obtain line profiles across the maps as needed.

9. The Sonix Flexscan software allows 3d surface and perspective views for data visualization. These are located in the ‘Process’ menu. For more detailed 3d visualizations, it is recommended to use 3rd-party software programs such as Visual Numerics PvWave or TableCurve 3d. To get the data off-line, an option in the surface profilometry window to ‘write ascii files’ is provided as mentioned in step 4.

REFERENCES

1. Stout, K.J., Sullivan, P.J., Dong, W.P., Mainsah, E., and Luo, N., Chapters 1 and 2, **The Development of Methods For The Characterisation of Roughness in Three Dimensions,** Publication no. EUR 15178 EN of the Commission of the European Communities.
2. **Surface Texture (Surface Roughness, Waviness, and Lay)**, ASME B46.1-1995.
3. Harding, K.G., Laser Scatter Surface Finish Measurement Techniques, **Laser Institute of America Proceedings of the Optical Sensing and Measurement Symposium – ICALEO’91,** Nov 3-8, 1991, Vol. 73, 1992.
4. Blessing, G.V. and Eitzen,D.G., Ultrasonic Sensor for measuring surface roughness, **SPIE Vol. 1009 Surface Measurement and Characterization** (1988).
5. FlexSCAN-C Ultrasonic C-Scan User’s Guide, Version 4, January 1998, Sonix, Inc., 8700 Morrissette Drive, Springfield, VA 22152.
6. Roth, D.J., Kiser, J.D., Swickard, S.M., Szatmary, S.M. and Kerwin, D.P., Quantitative Mapping of Pore Fraction Variations in Silicon Nitride Using an Ultrasonic Contact Scan Technique, **Res. Nondestr. Eval**., Vol. 6, 1995, pp. 125-168.
7. Roth, D.J., Hendricks, J.L., Whalen, M.F., Bodis, J.R. and Martin, K., Commercial Implementation of Ultrasonic Velocity Imaging Methods via Cooperative Agreement Between NASA Glenn Research Center and Sonix, Inc. NASA TM-107138, 1996.
8. Bevington, R.P., **Data Reduction and Uncertainty Analysis for the Physical Sciences**, Chapter 4, 1969. McGraw-Hill, New York, NY.
9. **Handbook of Physics and Chemistry**, 60th ed., CRC Press, pp. E-49 – E54.
10. **Nondestructive Testing Handbook**, second edition, Volume 7 Ultrasonic Testing, eds. Birks, A.S., Green, R.E., and Mcintire, P. American Society For Nondestructive Testing, 1991, p. 833.

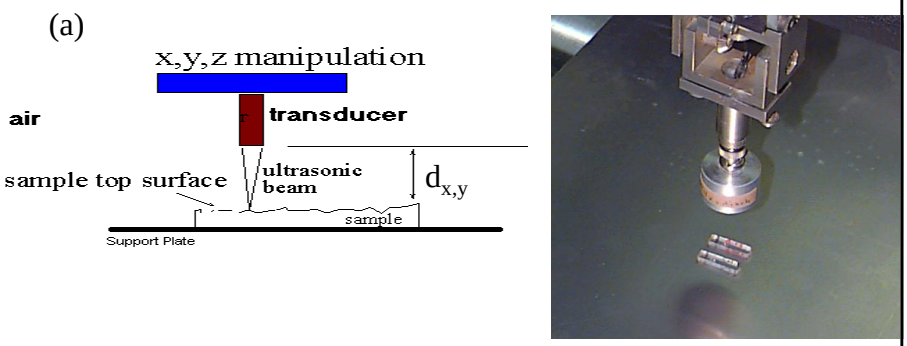

Figure 1. Experimental set-up for Air Surface Profilometry (a) Schematic of Basic Principle and set-up for plate samples (b) (next page) Instrumentation set-up.

Figure 1b. Instrumentation set-up

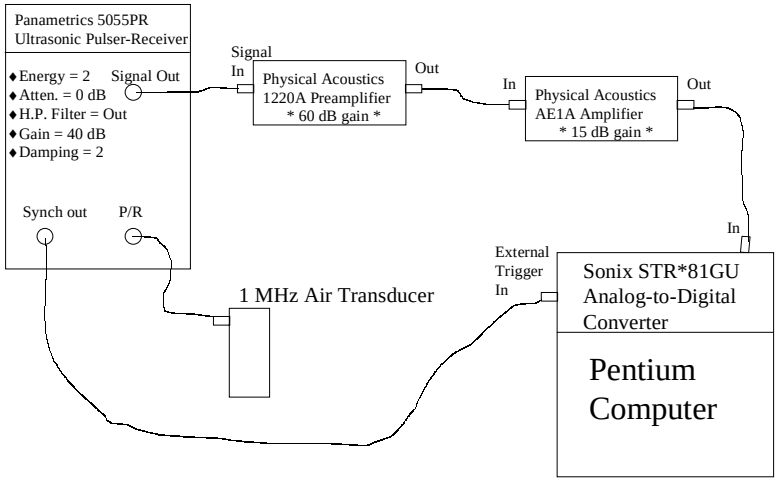

(a) (b)

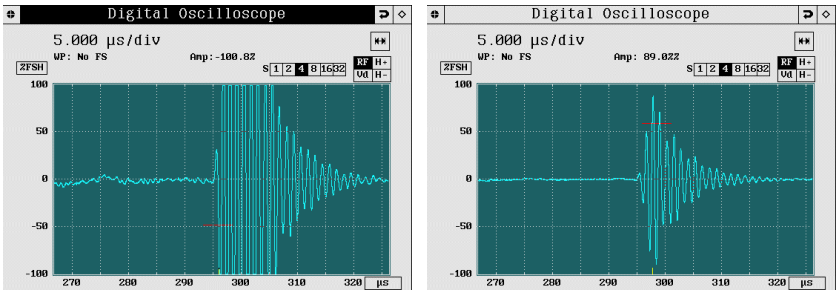

Fig. 2. Time gating options for air surface profilometry (a) gating leading edge of front surface echo (b) gating peak of front surface echo

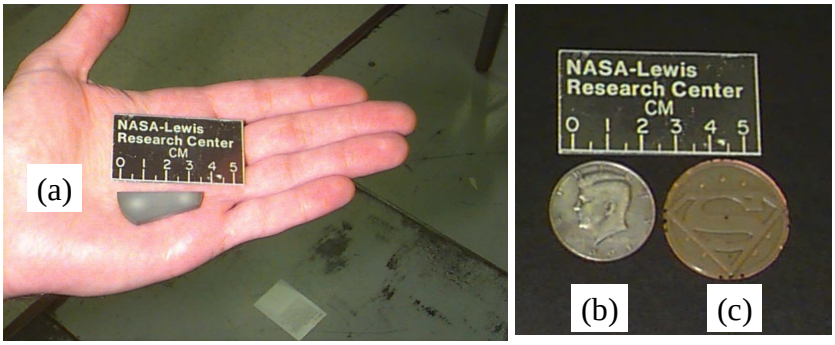

Fig. 3. Photos of proof-of-concept samples (a) ceramic wedge (b) Kennedy half-dollar coin (c) embossed superman logo

(a) (b)

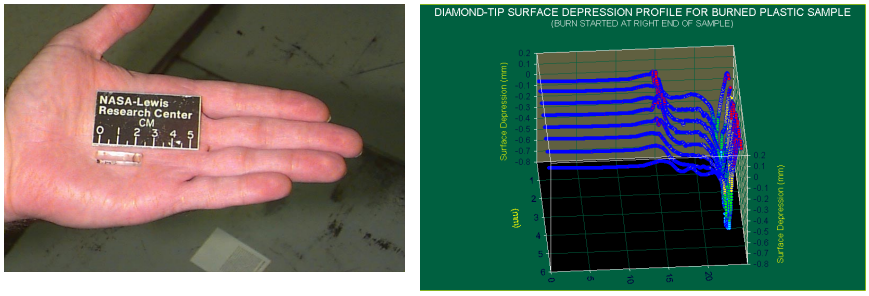

Fig. 4. Plastic sample that was the object in a microgravity combustion space experiment onboard the space shuttle (mission STS-54) (a) photograph (b) diamond tip profile

(a) (b) Manipulator Arm

Ultrasonic Air Transducer

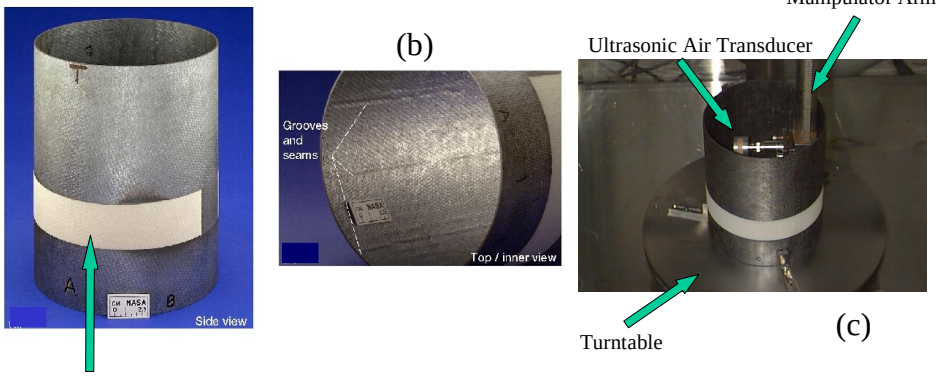

Turntable (c)

Protective Coating

Fig. 5. Ceramic composite cylindrical structure (a) side view showing protective coating (white strip), (b) inner view showing grooving (c) experimental set-up for inner surface profiling

Figure 6. Air Surface Profiles of Aluminum Step Wedge and Aluminum Channeled Sample for Determination of Depth and Lateral Resolution Capability of Air Surface Profilometry Used in This Investigation.

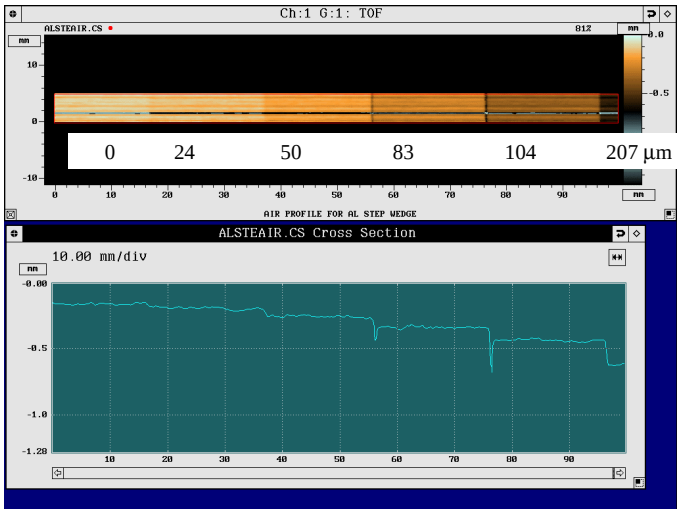

Fig. 6a. Air surface profile of aluminum step wedge showing the depth resolution available with the experimental set-up of this study is ~ 25 µm. Numbers above image indicate step depth in µm.

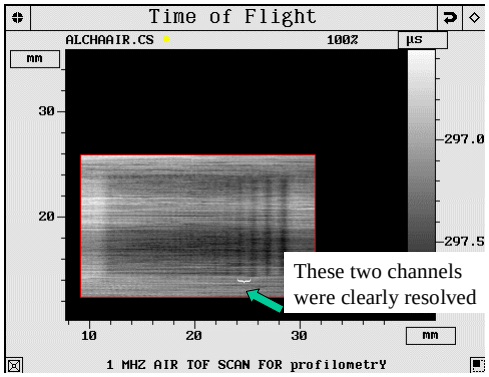

Fig. 6b. Time-of-flight image to front surface of aluminum channeled sample showing the lateral / spatial resolution available with the experimental set-up of this study is ~ 400 µm

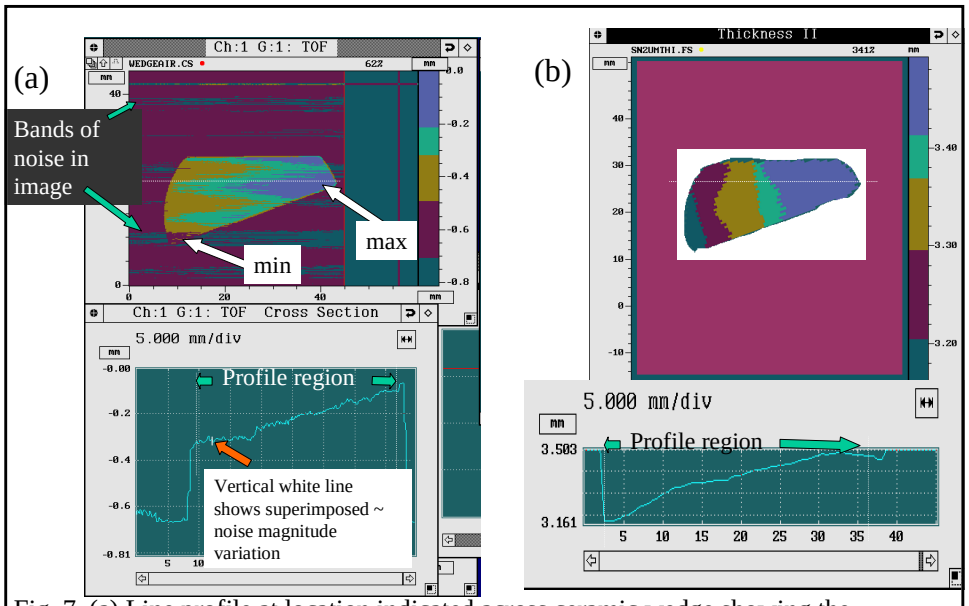

Fig. 7. (a) Line profile at location indicated across ceramic wedge showing the "roughness / noise" superimposed on the profile (b) "Smoother" line profile at location indicated across ceramic wedge for a thickness map obtained using through-thickness ultrasonic velocity measurements.

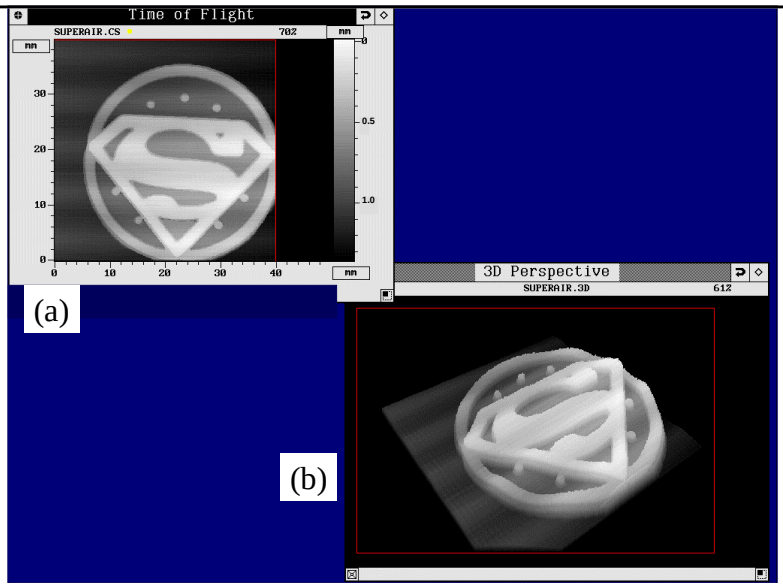

Fig. 8. Air surface profiles for plastic superman logo (a) Two-dimensional view (b) Three-dimensional view

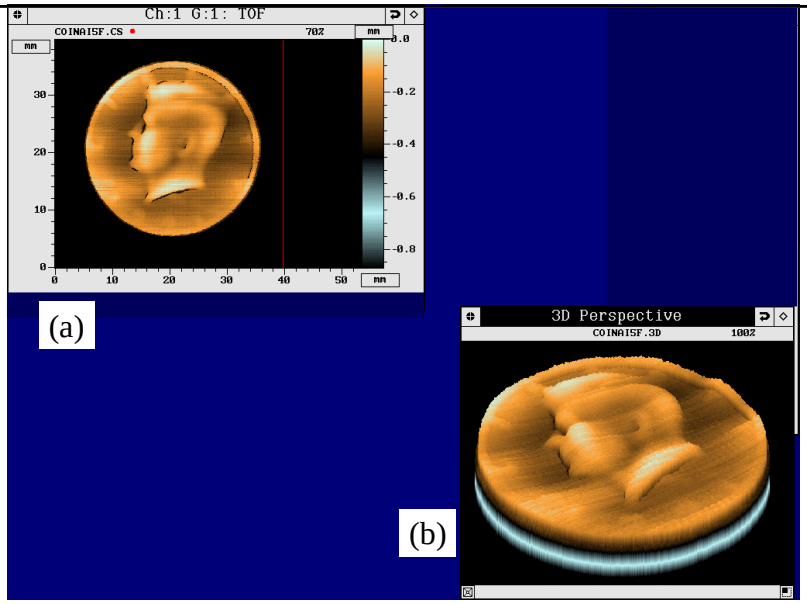

Fig. 9. Air surface profiles for Kennedy Half-dollar (a) Two-dimensional view (b) Three-dimensional view

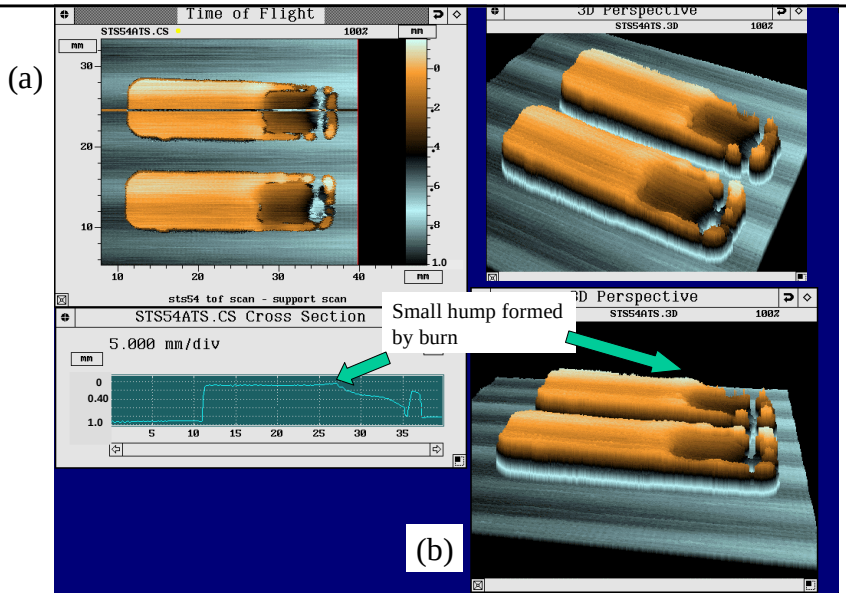

Fig. 10. Air surface profiles for Burned Space Experiment Samples (a) Two-dimensional view and line profile across one scan line of top sample (b) Three-dimensional view

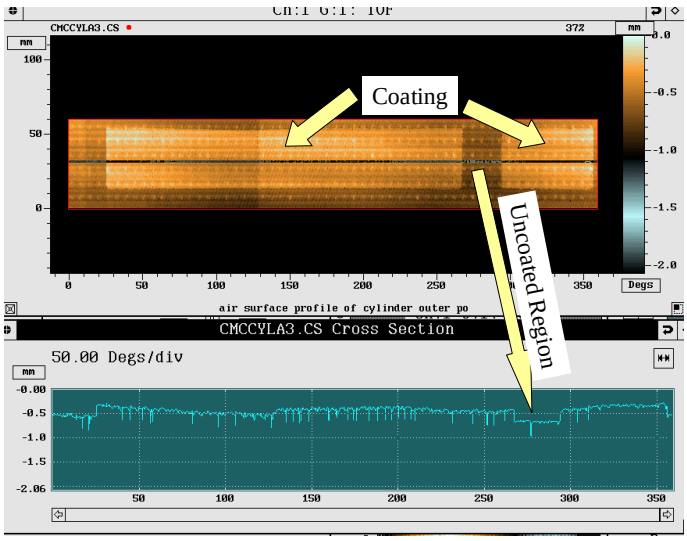

Fig. 11. Air surface profile of outer portion of cylindrical ceramic sample with line profile across one scan line. Shows difference in height between coated and uncoated regions.

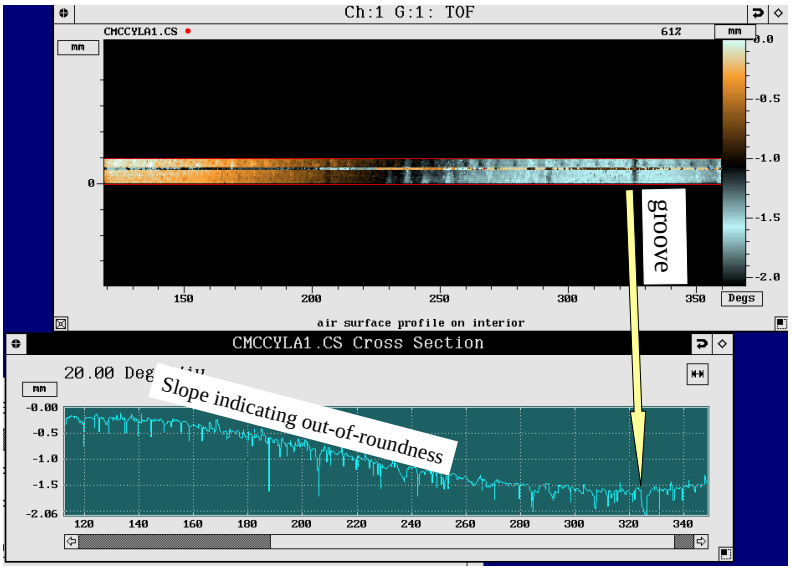

Fig. 12. Air surface profile of inner portion of cylindrical ceramic sample with line profile across one scan line. Shows grooves and tooling bump thickness variations on top of out-of-roundness condition (the latter indicated by the slope and is mainly due to set-up).

(a) (b)

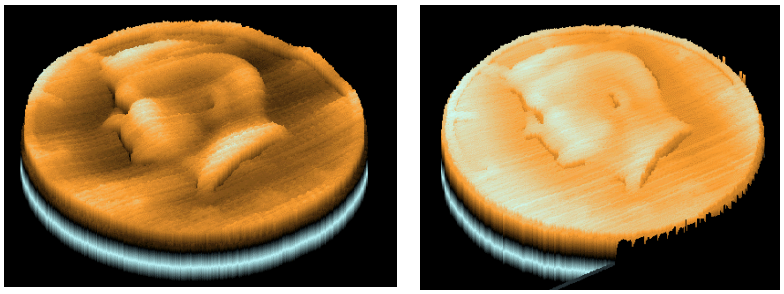

Fig.13. Comparison of air surface profiles scanned at (a) 5 mm/sec (b) 100 mm/sec

A1a

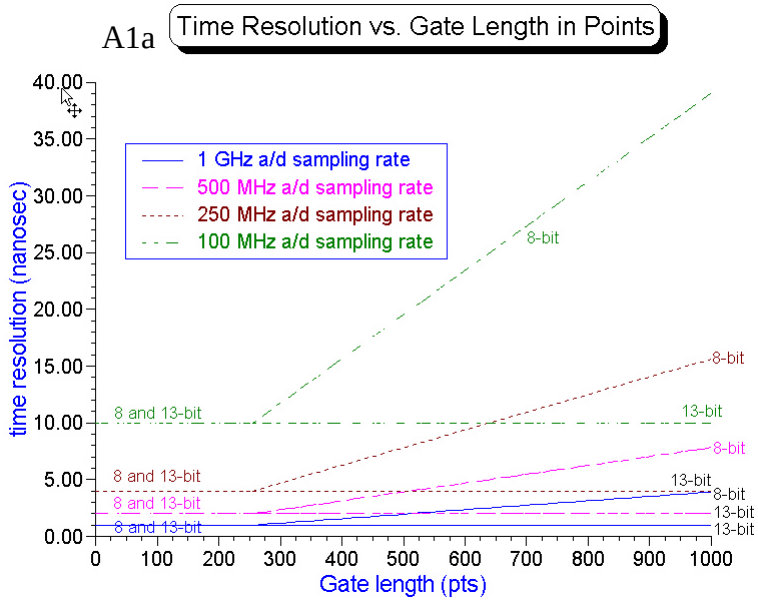

Fig. A1. Time resolution vs. Gate Length. (a) gate length in points (b) gate length in ηsec. Both figures show the gate lengths where time resolution begins to decrease beyond that set by the analog-to-digital sampling rate.

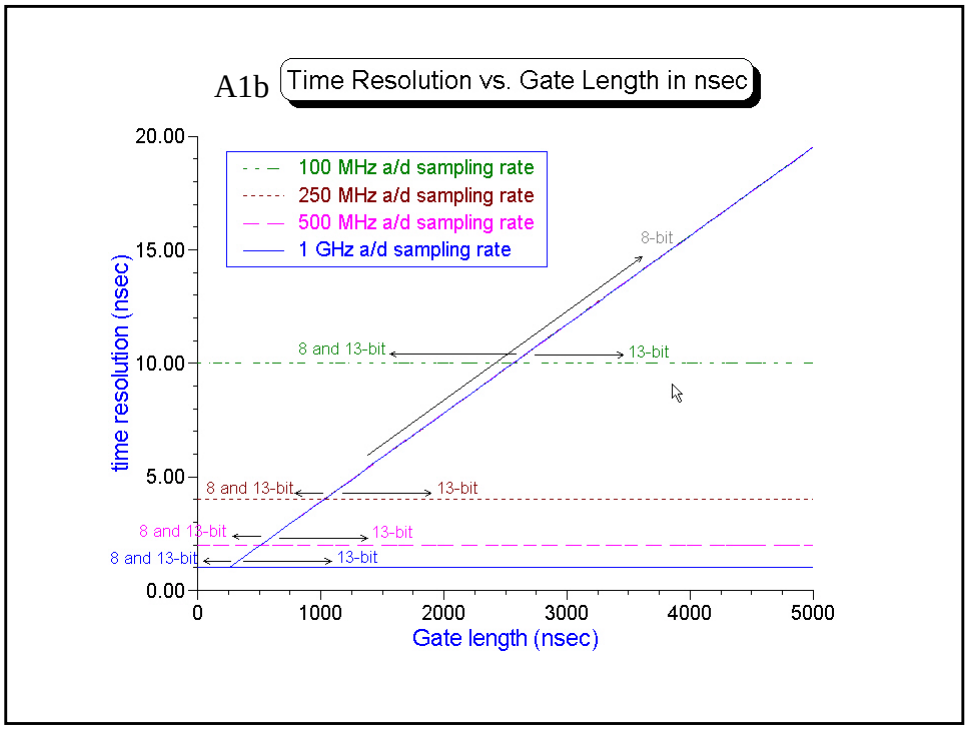

Fig. A2. Ultrasonic Velocity in Air vs. Temperature and Humidity

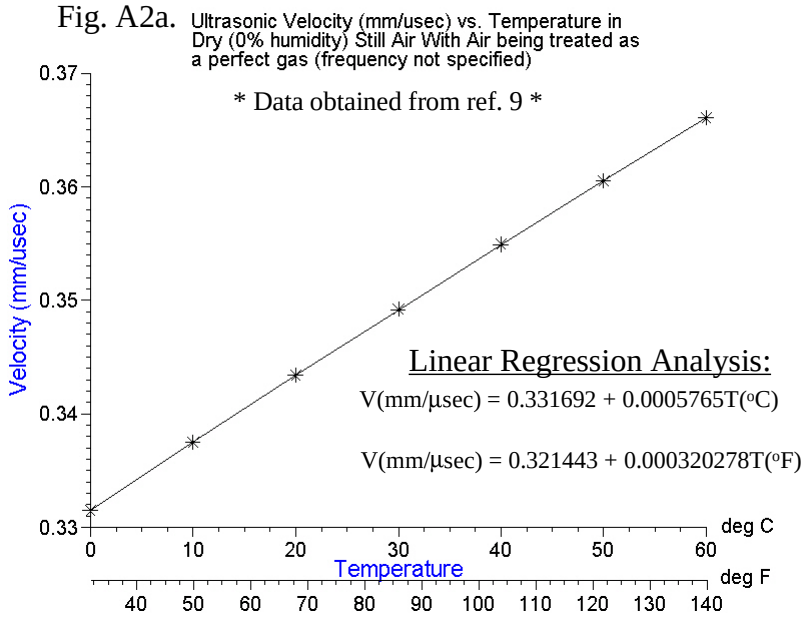

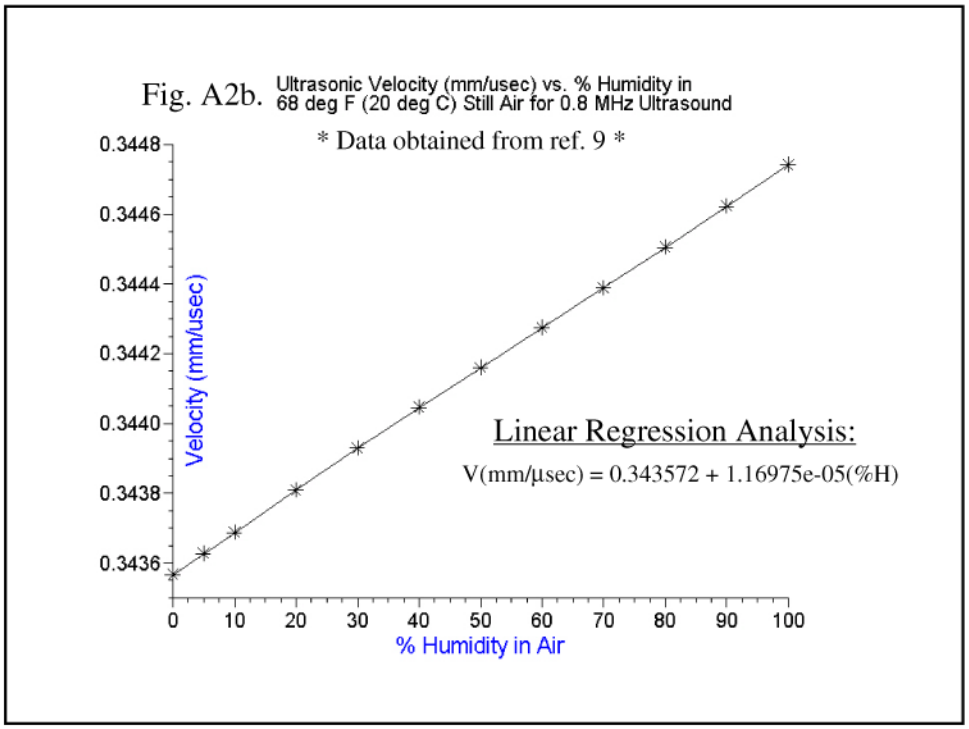

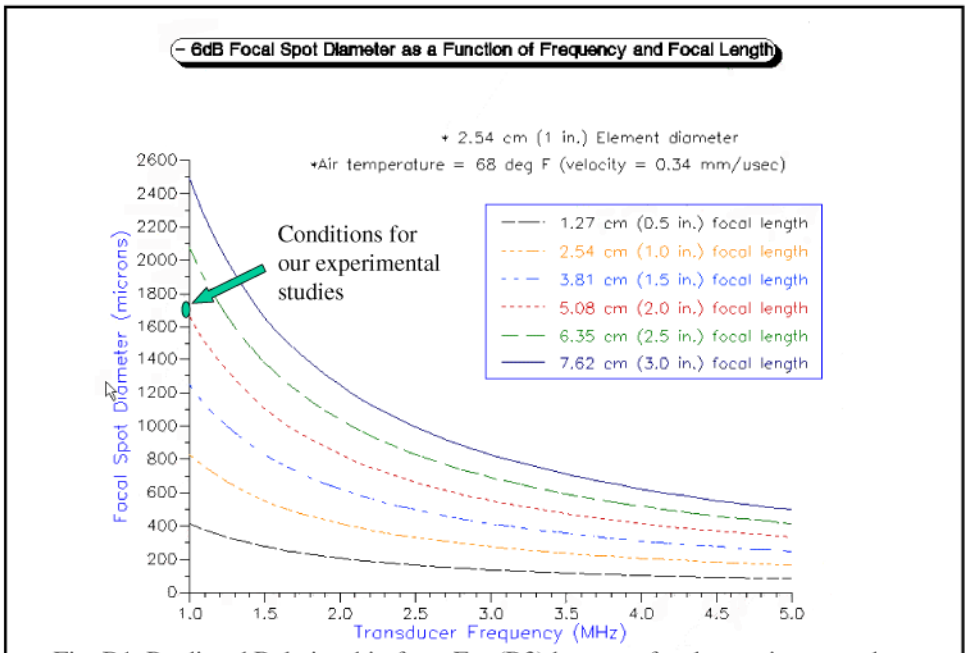

Fig. B1. Predicted Relationship from Eq. (B3) between focal spot size, transducer frequency, focal length, and element diameter for 2.54 cm element diameter

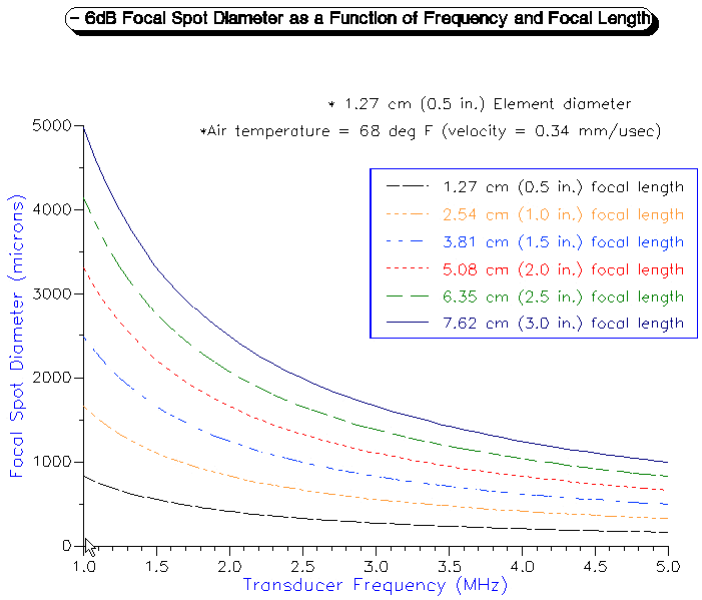

Fig. B2. Predicted Relationship from Eq. (B3) between focal spot size, transducer frequency, focal length, and element diameter for 1.27 cm element diameter

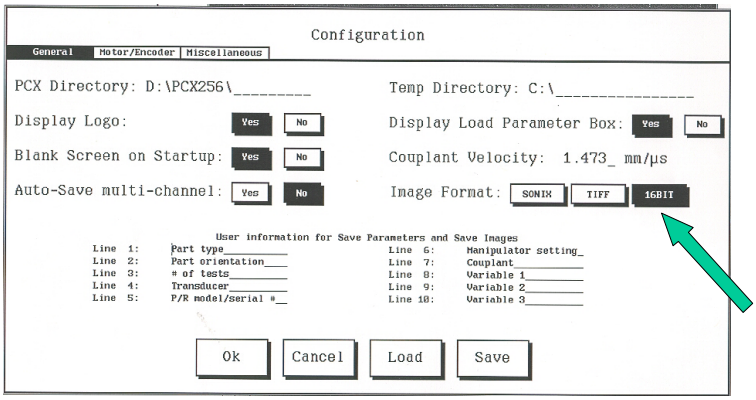

Fig. C1. Configuration window showing set-up for Image Format.

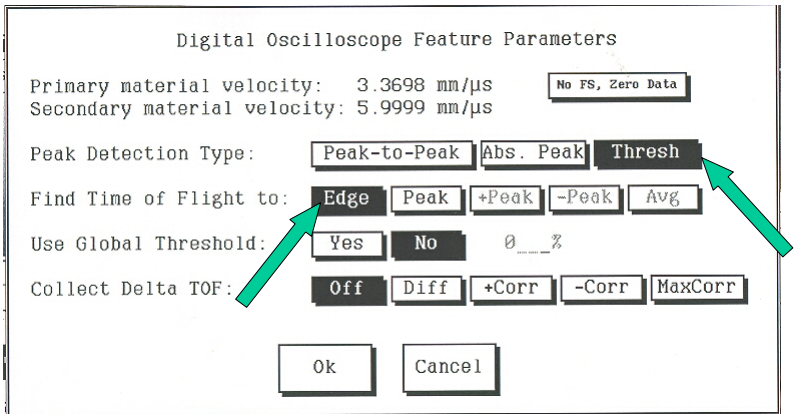

Fig. C2. Feature Parameters window showing set-up for waveform gating options.

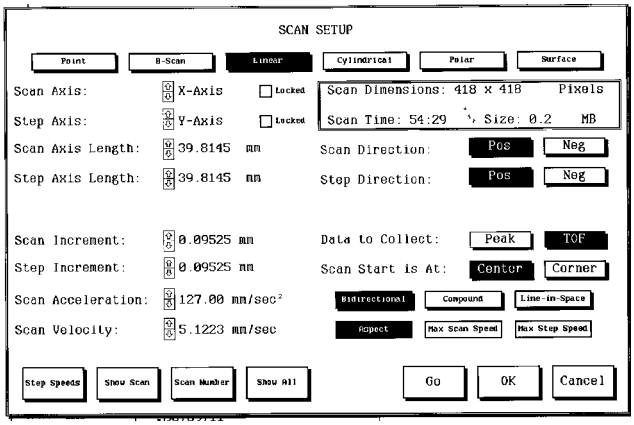

Fig. C3. Scan set-up window.

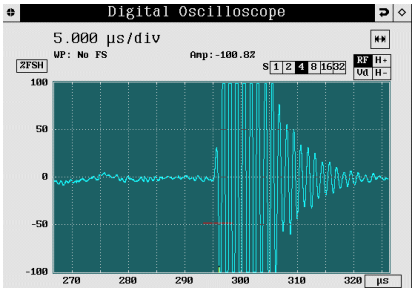

Fig. C4. Time gating leading edge of front surface echo.

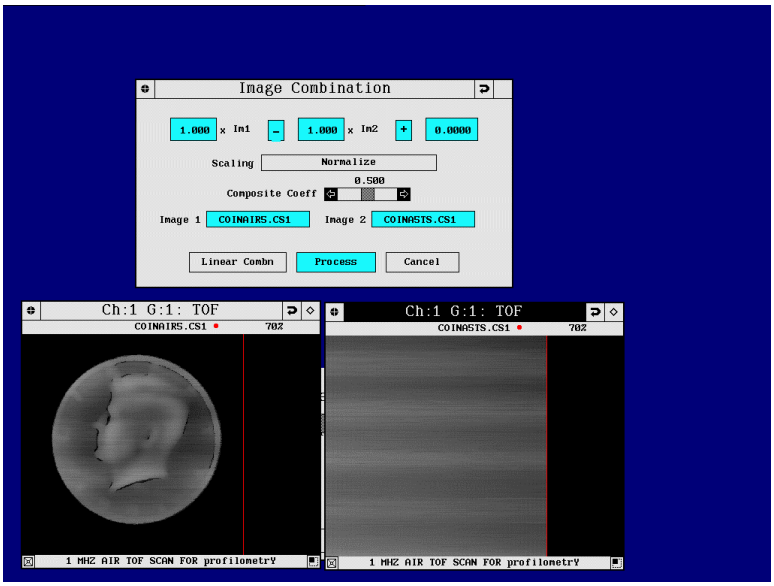

Fig. C5. Add/Subtract (Image Combination) Window for leveling.

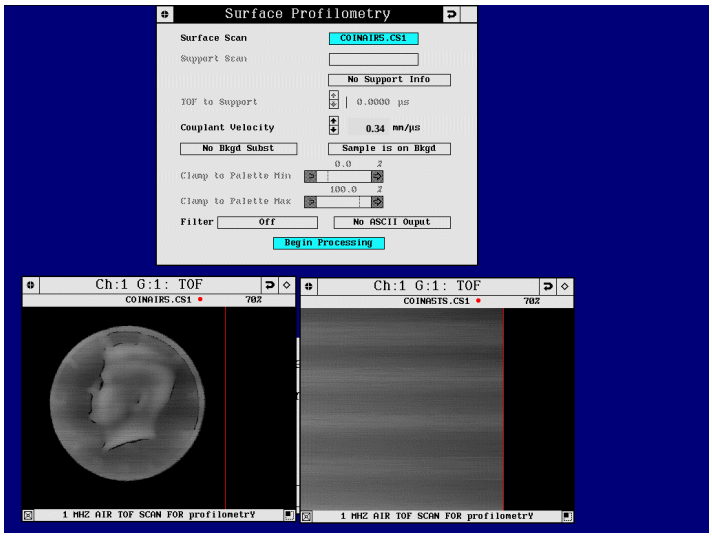

Fig. C6. Surface Profilometry Window.

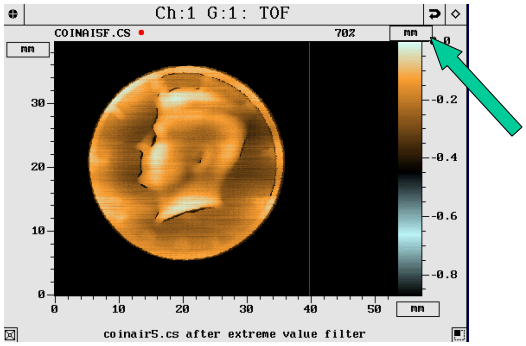

Fig. C7. Toggle the units in the upper right-hand corner to display profile in terms of time (µsec) or distance (mm or in.).

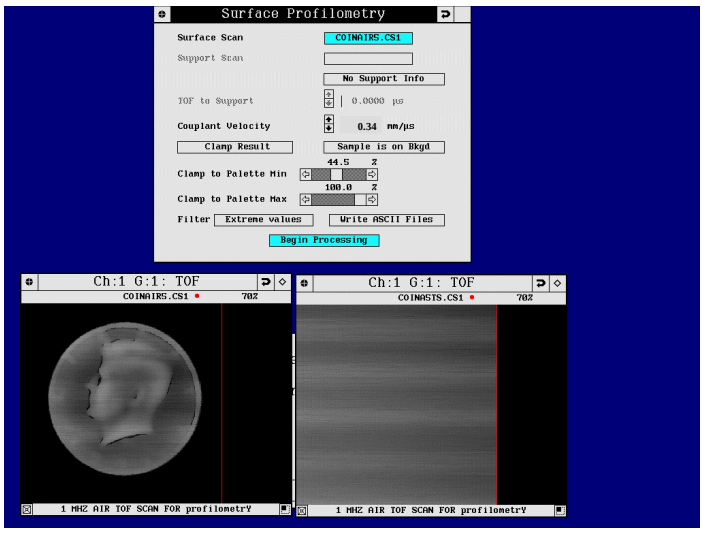

Fig. C8. Surface Profilometry Window showing extreme value filtering and write ascii files options.

REPORT DOCUMENTATION PAGE

Form Approved
OMB No. 0704-0188

Public reporting burden for this collection of information is estimated to average 1 hour per response, including the time for reviewing instructions, searching existing data sources, gathering and maintaining the data needed, and completing and reviewing the collection of information. Send comments regarding this burden estimate or any other aspect of this collection of information, including suggestions for reducing this burden, to Washington Headquarters Services, Directorate for Information Operations and Reports, 1215 Jefferson Davis Highway, Suite 1204, Arlington, VA 22202-4302, and to the Office of Management and Budget, Paperwork Reduction Project (0704-0188), Washington, DC 20503.

1. AGENCY USE ONLY (*Leave blank*)

2. REPORT DATE
May 1999

3. REPORT TYPE AND DATES COVERED
Technical Memorandum

4. TITLE AND SUBTITLE
3–D Surface Depression Profiling Using High Frequency Focused Air-Coupled Ultrasonic Pulses

5. FUNDING NUMBERS
WU–523–22–13–00

6. AUTHOR(S)
Don J. Roth, Harold E. Kautz, Phillip B. Abel, Mike F. Whalen,
J. Lynne Hendricks, and James R. Bodis

7. PERFORMING ORGANIZATION NAME(S) AND ADDRESS(ES)
National Aeronautics and Space Administration
John H. Glenn Research Center at Lewis Field
Cleveland, Ohio 44135–3191

8. PERFORMING ORGANIZATION REPORT NUMBER
E–11589

9. SPONSORING/MONITORING AGENCY NAME(S) AND ADDRESS(ES)
National Aeronautics and Space Administration
Washington, DC 20546–0001

10. SPONSORING/MONITORING AGENCY REPORT NUMBER
NASA TM—1999-209053

11. SUPPLEMENTARY NOTES
Don J. Roth, Harold E. Kautz, and Phillip B. Abel, NASA Glenn Research Center; Mike F. Whalen and J. Lynne Hendricks, Sonix, Inc. Springfield, Virginia 22152 (work funded under NASA Cooperative Agreement NCC3–489); James R. Bodis, Cleveland State University, 1983 E. 24th Street, Cleveland, Ohio 44115 (work funded under NASA Cooperative Agreement NCC3–304). Responsible person, Don J. Roth, organization code 5920, (216) 433–6017.

12a. DISTRIBUTION/AVAILABILITY STATEMENT
Unclassified - Unlimited
Subject Category: 38 Distribution: Nonstandard

This publication is available from the NASA Center for AeroSpace Information, (301) 621–0390.

12b. DISTRIBUTION CODE

13. ABSTRACT ***(Maximum 200 words)***
Surface topography is an important variable in the performance of many industrial components and is normally measured with diamond-tip profilometry over a small area or using optical scattering methods for larger area measurement. This article shows quantitative surface topography profiles as obtained using only high-frequency focused air-coupled ultrasonic pulses. The profiles were obtained using a profiling system developed by NASA Glenn Research Center and Sonix, Inc (via a formal cooperative agreement). (The air transducers are available as off-the-shelf items from several companies.) The method is simple and reproducible because it relies mainly on knowledge and constancy of the sound velocity through the air. The air transducer is scanned across the surface and sends pulses to the sample surface where they are reflected back from the surface along the same path as the incident wave. Time-of-flight images of the sample surface are acquired and converted to depth / surface profile images using the simple relation ($d = V*t/2$) between distance (d), time-of-flight (t), and the velocity of sound in air (V). The system has the ability to resolve surface depression variations as small as 25 μm, is useable over a 1.4 mm vertical depth range, and can profile large areas only limited by the scan limits of the particular ultrasonic system. (Best-case depth resolution is 0.25 microns which may be achievable with improved isolation from vibration and air currents.) The method using an optimized configuration is reasonably rapid and has all quantitative analysis facilities on-line including 2-D and 3-D visualization capability, extreme value filtering (for faulty data), and leveling capability. Air-coupled surface profilometry is applicable to plate-like and curved samples. In this article, results are shown for several proof-of-concept samples, plastic samples burned in microgravity on the STS-54 space shuttle mission, and a partially-coated cylindrical ceramic composite sample. Impressive results were obtained for all samples when compared with diamond-tip profiles and measurements from micrometers. The method is completely nondestructive, noninvasive, non-contact and does not require light-reflective surfaces.

14. SUBJECT TERMS
Nondestructive evaluation; Surface profilometry; Ultrasonics

15. NUMBER OF PAGES
38

16. PRICE CODE
A03

17. SECURITY CLASSIFICATION OF REPORT	18. SECURITY CLASSIFICATION OF THIS PAGE	19. SECURITY CLASSIFICATION OF ABSTRACT	20. LIMITATION OF ABSTRACT
Unclassified	Unclassified	Unclassified	